

# FE–BE COUPLING METHODS FOR ELASTOPLASTICITY

R. PERERA\* AND E. ALARCÓN

## 1. INTRODUCTION

Coupled finite element and boundary element methods are especially well suited for dealing with non-linear problems in an infinite half-space. The general technique of FE–BE coupling was developed in a classical paper by Zienkiewicz *et al.*<sup>1</sup>

Finite element and boundary element methods lead to very different kinds of systems: systems with sparse symmetric positive-definite matrices for FEM and systems with full non-symmetric matrices for collocation BEM. The first kind of systems may be solved efficiently by iterative methods, while the second kind is solved by direct methods. When general coupling is performed the result is a large matrix partially sparse but with full non-symmetric blocks, and neither a direct method nor an iterative one is convenient to solve such a system.

On the other hand, with the advent of modern multiprocessor computers, new approaches<sup>2</sup> have been pursued to produce novel numerical algorithms intrinsically parallelizable. In this way, the FEM–BEM coupling can be solved separately in the non-linear FEM region and in the linear BEM region, preserving the advantages of each method. Consistency of the subdomain problem with the original one is ensured by enforcing suitable transmission of information between adjacent subregions.

This paper presents a study about the different possibilities of performing the coupling in non-linear problems, as parallelizable as not parallelizable.

Numerical results are given which indicate the performance of the different proposed possibilities.

## 2. STANDARD BEM–NON-LINEAR FEM COUPLING

In cases such as soil plasticity a coupling method combining boundary and finite elements allows suitable simulation exploiting the best features of each method.<sup>3</sup>

In this case, the BEM region coincides with the infinite interface between both subregions, while the non-linear zone (FEM region) is massive. Since the non-linear zone is predominant to perform the coupling, we consider the boundary element region as an equivalent finite element.<sup>4</sup>

Considering separately the variables belonging to  $\Omega_1$  of the variables in the linear interface, coincident with  $\Omega_2$  ( $\Omega_2 \equiv \Gamma_I$ ) (Figure 1), the equilibrium equation in the FEM region is expressed as

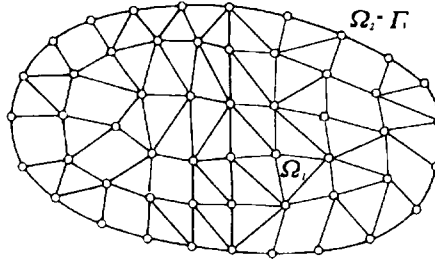


Figure 1. BEM–FEM coupling in an infinite half-plane

$$\begin{pmatrix} \mathbf{F}_{\text{int}}^1 \\ \mathbf{F}_{\text{int}}^2 \end{pmatrix} = \begin{pmatrix} \mathbf{F}_{\text{ext}}^1 \\ \mathbf{F}_{\text{ext}}^2 \end{pmatrix} \quad (1)$$

The boundary element system, without considering the body forces, is formulated in the interface  $\Omega_2 \equiv \Gamma_I$  as<sup>4</sup>

$$\mathbf{NG}^{-1}\mathbf{Hu}_2 = \mathbf{Nt}_2 \quad (2)$$

$\mathbf{H}$  and  $\mathbf{G}$  being coefficient matrices obtained using collocation nodal, and  $\mathbf{N}$  representing the Gram matrix. This is by no means a limitation of the method. Body forces or initial stresses derivable from a potential can be reduced to the boundary, as shown, for instance, in Rizzo.<sup>5</sup>

Adding (1) and (2), taking into account the equilibrium condition ( $\mathbf{t}_{11} = \mathbf{t}_{12}$ ) in the interface, the problem will be reduced to finding the displacements such that

$$\begin{aligned} \mathbf{F}_{\text{int}}^1 &= \mathbf{F}_{\text{ext}}^1 \\ \mathbf{F}_{\text{int}}^2 + \mathbf{Mu}_2 &= 0 \end{aligned} \quad (3)$$

where

$$\mathbf{M} = \mathbf{NG}^{-1}\mathbf{H} \quad (4)$$

The non-linear system in  $\Omega_1$  region can be solved iteratively with Newton's method. Linearizing system (3) about  $\mathbf{u}^k$  yields

$$\begin{pmatrix} \mathbf{A}_{11} & \mathbf{A}_{12} \\ \mathbf{A}_{21} & \mathbf{A}_{22} + \mathbf{M} \end{pmatrix}^k \begin{pmatrix} \Delta \mathbf{u}_1 \\ \Delta \mathbf{u}_2 \end{pmatrix}^k = \begin{pmatrix} \mathbf{R}_1 \\ 0 \end{pmatrix}^k \quad (5)$$

where

$$\mathbf{A}_{11} = (\mathbf{F}_{\text{int}}^1)'_{u_1} \quad \mathbf{A}_{12} = (\mathbf{F}_{\text{int}}^1)'_{u_2} \quad \mathbf{A}_{21} = (\mathbf{F}_{\text{int}}^2)'_{u_1} \quad \mathbf{A}_{22} = (\mathbf{F}_{\text{int}}^2)'_{u_2} \quad (6)$$

and the residual

$$\mathbf{R}_1 = \mathbf{F}_{\text{ext}}^1 - \mathbf{F}_{\text{int}}^1 \quad (7)$$

Solving (5) can be done in two different ways, taking into account the behaviour of the  $\Omega_2$  region. The first approach is summarized in Figure 2. In this approach the linear behaviour in  $\Omega_2$  is preserved, but all the systems are non-symmetric so the calculation is very expensive. The main disadvantage is eliminating the symmetry and the sparsity of  $\mathbf{A}_{11}$  obtained in the massive domain.

<pre> (i) <math>[\mathbf{A}_{11} - \mathbf{A}_{12}(\mathbf{A}_{22} + \mathbf{M})^{-1}\mathbf{A}_{21}]^k \Delta \mathbf{u}_1^k = \mathbf{R}_1^k</math> (ii) <math>\mathbf{u}_1^{k+1} = \mathbf{u}_1^k + \Delta \mathbf{u}_1^k</math> (iii) <math>\mathbf{R}_1^{k+1} = (\mathbf{F}_{\text{ext}}^1) - (\mathbf{F}_{\text{int}}^1)^{k+1}</math> (iv) if <math>\ \mathbf{R}_1^{k+1}\  &gt; \text{TOL}</math> then       <math>k \leftarrow k + 1</math>       goto (i)     else       goto (v)     endif (v) <math>(\mathbf{A}_{22} + \mathbf{M})\Delta \mathbf{u}_2 = -\mathbf{A}_{21}\Delta \mathbf{u}_1</math> </pre>
---

Figure 2. Standard coupling preserving the linearity of the interface

<pre> (i) <math>[\mathbf{A}_{22} + \mathbf{M} - \mathbf{A}_{21}\mathbf{A}_{11}^{-1}\mathbf{A}_{12}]^k \Delta \mathbf{u}_2^k</math> <math>= [-\mathbf{A}_{21}\mathbf{A}_{11}^{-1}\mathbf{R}_1]^k</math> (ii) <math>\mathbf{A}_{11}^k \Delta \mathbf{u}_1^k = [\mathbf{R}_1 - \mathbf{A}_{12}\Delta \mathbf{u}_2^k]^k</math> (iii) <math>\mathbf{u}_2^{k+1} = \mathbf{u}_2^k + \Delta \mathbf{u}_2^k</math> (iv) <math>\mathbf{u}_1^{k+1} = \mathbf{u}_1^k + \Delta \mathbf{u}_1^k</math> (v) <math>\mathbf{R}_1^{k+1} = (\mathbf{F}_{\text{ext}}^1) - (\mathbf{F}_{\text{int}}^1)^{k+1}</math> (vi) if <math>\ \mathbf{R}_1^{k+1}\  &gt; \text{TOL}</math> then       <math>k \leftarrow k + 1</math>       goto (i)     else       exit     endif </pre>
--

Figure 3. Standard coupling enforcing the non-linearity in the interface

The second approach to solving (5) is orientated to preserving the symmetry and sparsity of  $\mathbf{A}_{11}$ . To attain this we solve the  $\Omega_2$  region as a non-linear region, i.e. iteratively. This approach is summarized in Figure 3. The main advantage of this approach is the possibility of solving the symmetric problems iteratively (non-linear problems in the massive domain) by a preconditioned conjugate gradient method. Despite several systems having to be solved iteratively, the process is not too time-consuming because  $\mathbf{A}_{12}$  is generally sparse and the preconditioning is performed only once. However, the main disadvantage consists of applying the Newton–Raphson iterations to solve a linear region  $\Omega_2$ .

Of the two possibilities (Figures 2 and 3), the second approach produces in the massive region  $\Omega_1$  symmetric and sparse systems which decrease the cost of the resolution. For this reason, we use this second approach to obtain results when a standard coupling is performed.

### 3. INTERFACE RELAXATION PROCEDURE

Another approach to performing the BEM–FEM coupling is based on the decomposition of the initial problem into two subdomains. By this procedure, we solve the differential equations in

separate mesh resolutions and iterate between subdomains until convergence is reached at the BEM–FEM interface.<sup>6,7</sup> It yields a family of almost independent subproblems of lower computational complexity.

This approach allows for the separate treatment of the linear and non-linear problems, keeping the advantages of both the BEM and FEM methods.

Consistency of the subdomain problem with the original one is ensured by enforcing suitable transmission of information between adjacent subregions using compatibility and equilibrium. To achieve convergence, at each iteration a relaxation is accomplished at the subdomain interface.<sup>15</sup>

In this approach a Dirichlet problem in the interface is solved by the BEM method and a Neumann problem in the interface is solved in the non-linear FEM subdomain (Dirichlet–Neumann method). The tractions obtained with the BEM method are used as boundary conditions in the FEM region. On the other hand, the Dirichlet boundary conditions in the BEM domain are obtained through a relaxation at the interface,

$$\mathbf{u}^{(\text{BEM})^{k+1}} = \theta \mathbf{u}^{(\text{FEM})^k} + (1 - \theta) \mathbf{u}^{(\text{BEM})^k} \quad (8)$$

$\mathbf{u}^{(\text{FEM})^k}$  and  $\mathbf{u}^{(\text{BEM})^k}$  being the available displacements in the  $k$ th iteration for the two subdomains, and  $0 < \theta < 1$  a relaxation parameter.

The relaxation parameter  $\theta \in ]0, 1[$  can be constant or selected dynamically<sup>8</sup> by means of a simple formula to maximize the rate of convergence of the above iteration by a subdomain procedure.

From the concept of the Steklov–Poincaré operator,<sup>9</sup> the iteration-by-subdomain method can be interpreted in different ways: as a successive under-relaxation method in the interface or as a preconditioned conjugate gradient method.

#### 4. PRECONDITIONING

Newton’s method is very attractive for solving a system of non-linear equations, but it may be extremely expensive because it requires the solution of a linear system at each iteration step. An alternative way of improving the efficiency of Newton’s method when it is used in large systems is by a composite Newton–preconditioned conjugate gradient (PCG)<sup>10</sup> technique for the linearized system in lieu of the conventional LDU factorization of the global tangent operator.

As a preconditioner we use the tangent operator<sup>11</sup>  $\mathbf{K}_{T0} = -[(\mathbf{F}_{\text{int}}^1)_{,u_1}']^1$  during the first iteration of every load step. This preconditioner has the typical advantages and disadvantages of Newton’s method;  $\mathbf{K}_{T0}$  contains information on the present value of the load step; the method would be direct during the first iteration due to the necessary factorization of the preconditioner.

#### 5. NUMERICAL RESULTS

In this Section we compare the performance of each of these coupling algorithms. The code used in the present study is an enhanced non-linear version of DLEARN<sup>12</sup> in which we have incorporated the boundary elements. All computations were performed in double precision on a SPARCstation 2 supercomputer. The closest-point projection algorithm<sup>13</sup> coupled with the Drucker–Prager elastoplastic model was used to construct the stress field. The tangent stiffness matrix was obtained from the consistent tangent elastoplastic moduli<sup>14</sup> using an associated flow rule.

Convergence of the non-linear algorithm is measured in terms of the residual norm with an error tolerance of  $10^{-3}$ . The error tolerance for the PCG secondary iterations is  $10^{-2}$ . Material responses are sampled at the Gauss points using a nine-point integration in two-dimensional quadrilateral elements.

### 5.1. Plane strain example

As an example we consider the effects of initial stresses on a perforation with a horseshoe-like geometry at a depth of 60 m with an inner radius of 5 m. The infinite half-plane modelled by boundary elements is located at a distance three times the radius. Two-dimensional quadratic finite elements and one-dimensional quadratic boundary elements are employed. For simplicity, we consider a homogeneous material with the following constants: Young's modulus  $E = 2.5 \times 10^6 \text{ t/m}^2$ , Poisson's ratio  $\nu = 0.27$ , and density  $\gamma = 2.4 \text{ t/m}^3$ ; the unconfined compression strength  $R_c$  is  $2240 \text{ t/m}^2$  and the angle of internal friction  $\phi = 33^\circ$ . Initial stresses were generated internally at each integration point and after an internal pressure was used to proceed with the computations.

It is interesting to study the performance of the coupling algorithm when the mesh is refined progressively. For this reason, two different meshes are employed in the calculations (Figures 4(a) and (b)). These two meshes have 864 and 1320 degrees of freedom, respectively. The calculations reported here were performed in four different load steps, and four alternative algorithms were employed:

- (a) a traditional coupling algorithm (Figure 3) with the full Newton method employing Crout triangular factorization for direct equation solving (TRAD-NR-D)
- (b) a traditional coupling algorithm (Figure 3) with the composite Newton-PCG iteration (TRAD-NR-PCG)
- (c) coupling by the Dirichlet-Neumann relaxation procedure with the full Newton method employing Crout triangular factorization for direct equation solving. The relaxation parameter is selected dynamically (RELAJ-NR-D)
- (d) coupling by the relaxation procedure with the composite Newton-PCG iteration with a dynamic relaxation parameter (RELAJ-NR-PCG).

Tables I and II summarize the performance of each of the four algorithms for the two different meshes. When a relaxation procedure is used, we prefix three relaxation iterations in each load step.

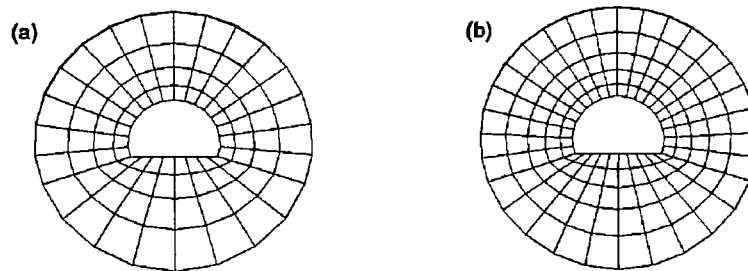


Figure 4. (a) Mesh 1 (864 dof); (b) mesh 2 (1320 dof)

Table I. Excavation (mesh 1–864 dof)

Criteria	TRAD-NR-D	TRAD-NR-PCG	RELAJ-NR-D	RELAJ-NR-PCG
No. load steps	4	4	4	4
No. global iterations	21	21	52	51
No. relaxat. iterations	–	–	12	12
No. global iter./step	5.25	5.25	13	12.75
No. global iter./relax. iter.	–	–	4.33	4.25
No. factorizations	21	4	52	12
No. subiterations	–	1451	–	186
No. subiter./global iter.	–	69.09	–	3.65
Total CPU (s)	1232.05	1749.95	929.969	690.031

Table II. Tunnel excavation (mesh 2–1320 dof)

Criteria	TRAD-NR-D	TRAD-NR-PCG	RELAJ-NR-D	RELAJ-NR-PCG
No. load steps	4	4	4	4
No. global iterations	19	20	50	50
No. relax. iterations	–	–	12	12
No. global iter./step	4.75	5	12.5	12.5
No. global iter./relax. iter.	–	–	4.17	4.17
No. factorizations	19	4	50	12
No. subiterations	–	1641	–	174
No. subiter./global iter.	–	82.05	–	3.48
Total CPU (s)	2882.05	4154.98	1881.06	1325.98

The results show that the relaxation procedures require less CPU compared with the standard coupling methods. This is more evident when the number of degrees of freedom increase. In the standard methods it is necessary, in each Newton iteration, to solve the subsystems in  $\mathbf{A}_{11}^{-1}\mathbf{A}_{12}$ , which increase progressively with the number of non-null columns in  $\mathbf{A}_{12}$  and hence with the degrees of freedom.

For the relaxation method, the PCG is better than Crout's factorization since it is only necessary to solve the system  $\mathbf{A}_{11}\Delta\mathbf{u}_1 = \mathbf{R}_1$  in each Newton iteration, and the number of Crout's factorizations is less when the PCG is used. So the RELAJ-NR-PCG is the least expensive of all the proposed coupling possibilities.

### 5.2. Relaxation parameter

In all the calculations we have adopted a dynamic relaxation parameter.<sup>8</sup> In Table III we summarize the results obtained when a constant parameter is used during all the process in lieu of

Table III. Performance of the relaxation algorithm for different values of  $\theta$ 

	$\theta$ DYNAMIC	$\theta = 0.1$	$\theta = 0.3$	$\theta = 0.5$	$\theta = 0.7$
No. load steps	4	4	4	4	divergence
No. global iterations	52	46	48	73	divergence
No. global iter./step	13	11.5	12	18.25	divergence
Total CPU (s)	323.97	286.84	299.32	408.498	divergence

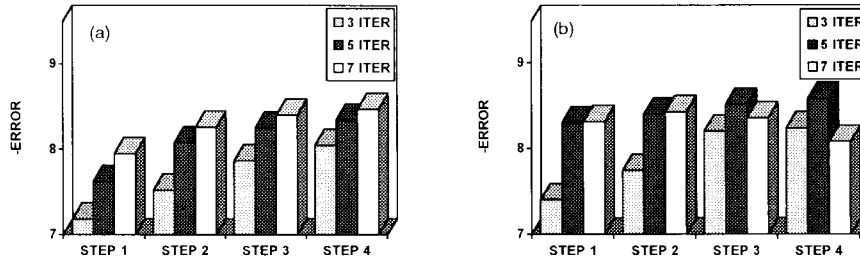


Figure 5. Evolution of ERROR with the number of relaxation iterations: (a)  $\theta = 0.3$ ; (b)  $\theta$ -dynamic

a dynamic parameter. It can be observed that  $\theta$ -values less than 0.5 are suitable, while higher values are slower and the algorithm can even diverge.

We have predetermined three relaxation iterations in each load step. This conclusion is obtained from previous tests. If we denote by ERROR the natural logarithm of the maximum among the errors at the interfaces between the BEM solution and the FEM solution in the same relaxation iteration, then we can represent ERROR with the number of relaxation iterations. For this, we have chosen a constant value  $\theta = 0.3$  (Figure 5(a)) and a  $\theta$ -dynamic (Figure 5(b)).

From the observation of Figure 5(b) we can deduce that a higher number of iterations does not produce better accuracy when a  $\theta$ -dynamic is employed. However, when we use a constant parameter (Figure 5(a)), the accuracy increases with the number of iterations, but this better accuracy probably does not compensate the higher cost.

## 6. CONCLUSIONS

Different FEM–BEM coupling algorithms have been investigated in a non-linear context over an infinite half-plane. In addition to the traditionally used ways, we have proposed a different alternative based on solving the BEM and FEM domains separately. This allows us to decouple the non-linear and linear equations and solve the subproblems independently, therefore allowing parallel computations within any multiprocessor environment.

Referring to the first approach (standard coupling), from a computational point of view, the enforcement of the linear half-plane as a non-linear domain has turned out to be more efficient since it allows for the preservation of the symmetry and sparsity of the FEM matrix. The second approach, the relaxation procedure, has been more optimal in CPU time. This would have been even more evident if a multiprocessor computer had been used.

The choice of the  $\theta$  relaxation parameter has been important to guarantee the convergence of the method. Values less than 0.5 or dynamic have been necessary for this reason.

A comparison between the conventional LDU factorization of the global tangent operator and the iterative methods based on preconditioned conjugate gradients (PCG) for solving large systems of equations associated with a linearized problem has been developed. We have shown that the composite Newton–PCG technique has considerable potential for usefulness in large-scale computations.